Reduced Kinetic Models for the Combustion of Jet Propulsion Fuels

Stephen Dooley[1+], Frederick L. Dryer[2#], Tanvir I. Farouk[3†], Yiguang Ju[2#], Sang Hee Won[2*]

[1]*Department of Chemical and Environmental Sciences, University of Limerick, Ireland*
[2]*Department of Mechanical and Aerospace Engineering, Princeton University, Princeton, NJ, USA*
[3]*Department of Mechanical Engineering, University of South Carolina, Columbia, SC, USA*

Reduced chemical kinetic models to predict the combustion characteristics of jet propulsion fuels are produced and tested. The parent detailed kinetic model has been developed on the basis of a surrogate fuel formulation methodology that utilizes combustion property targets measured for a particular real fuel to formulate a chemical mixture of n-alkanes, iso-alkanes and aromatic functionalities to emulate the combustion behavior of specific target jet aviation fuels. Detailed model predictions are compared against reflected shock ignition delays of both pure components and surrogate fuel mixtures. Systematically reduced models for each individual fuel component are produced and used to test the parent model performance against laminar burning velocity. Finally, a range of systematically reduced kinetic models for two, substantially different, validated surrogate fuels for a particular jet aviation fuel are produce and tested to allow the user a choice in computational cost versus reduced model fidelity. A reduced model of 233 species is produced that closely shares the predictability of the detailed model over the tested conditions. Analysis of the models provides a basis for further refinements in describing the chemical kinetic behavior of all conventional and alternative jet fuels. The limitations of the presented approach are discussed and needs for further refinements are identified.

I. Introduction

FORMULATION methodologies of appropriate surrogate mixtures that emulate the combustion behaviors of a real aviation fuel have been extensively investigated by various approaches in the last decade [1-14]. Recently, it has been demonstrated that successful surrogate mixtures for the emulation of combustion kinetic behaviors can be formulated by matching select physical and chemical properties of a targeted fuel [12-14]. These studies have utilized the Derived Cetane Number (DCN), hydrogen to carbon molar ratio (H/C ratio), average molecular weight (MW), and the Threshold Sooting Index (TSI) as fundamental metrics to qualify the properties of transportation fuels that are important to the occurrence of combustion phenomena that are kinetic in nature. Based on this methodology, two surrogate mixtures have been formulated targeting a specific jet fuel, Jet-A POSF 4658. The first generation Jet-A POSF 4658 surrogate [12] is comprised of a mixture of n-decane, iso-octane, and toluene (n-decane/iso-octane/toluene 42.7/33.0/24.3 mole %). In order to additionally match the mean molecular weight and threshold sooting index of the target fuel, a second generation Jet-A POSF 4658 surrogate has been formulated [13] composed of the heavier components, n-dodecane, n-propyl benzene, and 1,3,5-trimethyl benzene in addition to iso-octane (n-dodecane/iso-octane/1,3,5 trimethyl benzene/n-propyl benzene 40.41/29.48/7.28/22.83 mole %). To provide ground truth information, the goodness of these formulated

[+] Senior Research Scientist, Dept. of Chem. & Environ. Sciences, University of Limerick, Member of AIAA
[#] Professor, Dept. of Mech. & Aero. Eng., Princeton University, Fellow of AIAA
[†] Assistant Professor, Dept. of Mech. Eng., University of South Carolina, Member of AIAA
[*] Research Scholar, Dept. of Mech. & Aero. Eng., Princeton University, Member of AIAA

surrogates has been ascertained by entirely experimental comparisons of the combustion properties of real and surrogate fuels. Such experimental tests have been performed in various facilities to cover a broad range of pertinent pressures, temperatures, combustion phenomena and timescales; 1) global reactivity profiles in a variable pressure flow reactor, 2) ignition delay measurements in a shock tube (ST) and a rapid compression machine, 3) laminar burning velocities, extinction limits of nonpremixed (4) and premixed (5) counterflowing flames, 6) detailed intermediate species measurements in high temperature, high pressure shock tube oxidation studies and 7) semi-detailed soot profiles in laboratory burner stabilized flames [12, 13].

In all cases, at all conditions, the measured behaviors of surrogate fuels and real fuel were found to be qualitatively similar, and with some minor exceptions at some test conditions. More generally, the behaviors are quantitatively indistinguishable at the global level [13]. An explanation for the similarity in these extensive experimental comparisons founded by functional group additivity has been proposed by the provision in each fuel for the formation of a common pool of reactivity controlling intermediate species rather than the fuels initial detailed chemical composition.

The objective of present study is to demonstrate the performance of a fundamentally constructed chemical kinetic model to numerically reproduce the behavior of both formulated surrogate mixtures in the global combustion phenomena of ignition delay and laminar burning velocity as two important initial performance targets for aviation gas turbine applications.

The detailed chemical kinetic model is first tested against such available homogeneous mixture measurements of each pure component. A multitude of reduced models for each pure component are produced from the parent detailed model and tested against the available laminar burning velocity data of each surrogate fuel component.

The same procedure is employed to test the model performance against the ignition delay and burning velocity data of the surrogate mixtures presented in [12-13]. Finally, the reader is presented with a number of reduced kinetic models ranging in content from, very many species, valid to the state of the art at the highest available level of fidelity at a broad range of conditions, to very few species, valid to a lesser degree of fidelity at a narrower range of conditions. Testing of these reduced models allows for the identification of the smallest model to retain the fidelity of the detailed parent model over a large range of conditions. This approach is particularly beneficial for evaluating the potential of the present paradigm for the combustion modeling of real liquid transportation fuel in computational fluid dynamics applications.

II. Experimental

Kinetic Model Construction

A detailed chemical kinetic model for both the 1st generation and 2nd generation Jet-A POSF 4658 surrogate fuels has been assembled. The surrogate fuel chemistry is described by using the recent aromatic chemistry sets of Metcalfe et al. [15], Won et al. [16] and Diévart et al. [17] for toluene, n-propyl benzene and 1,3,5-trimethyl benzene respectively. These assemblies are extensions of one another, entirely self-consistent in construction. Thus, the performance demonstrated in each supporting work is expected to be implicitly valid in the surrogate model performance described here.

The C_0-C_4 sub-mechanism that forms the basis for these pure component chemical kinetic models and the surrogate fuel models herein described is that which was assembled and tested for toluene oxidation [15]. In summary it consists of the H_2/O_2 [18] and C_1 chemistry of Zhao et al. [19] up to and inclusive of the reaction $CH_3 + CH_3 (+M) = C_2H_6 (+M)$. The ethane consumption and higher hydrocarbon chemistry is described by a C_2 to C_4 sub-mechanism that was tested by Healy et al. [20]. The description of the base chemistry is completed by the incorporation of the work of Laskin et al. [21] which describes the higher alkenyl type species, such as butadiene.

The higher *n*-alkane chemistry of Westbrook et al. [22] has been adopted for n-alkanes from n-pentane up to and inclusive of n-dodecane. The *iso*-alkane chemistry of Mehl and co-workers [23] is adopted to

describe the oxidation of iso-octane and related iso-alkenyl species of carbon numbers greater than four. So called *cross-reactions* involving the interaction of high molecular weight fuel radicals or intermediates from the different generic functional classes are not considered in the kinetic model, which only allows fuel components to interact through their respective influence on the small species population. This assumption is consistent with the experimental observations presented in [12-13] which showed no evidence of the occurrence of such processes to a measurable degree, leading to a conclusion that the occurrence of such reactions does not perturb the reactivity of the chemical system at all significantly in such oxidizing environments[13].

In the case where there has been a conflict or duplication of nomenclature, chemistry or thermodynamic parameters between the individual component sub-models, chemical reaction, rate constant and thermodynamic parameters have been chosen in the following order of preference; Metcalfe et al. (Won et al., Dievart et al.) > Mehl et al.> Westbrook et al. Careful attention has been taken to ensure that each submodel is properly compatible at the interface C_4-C_5 chemistry level. A Lennard-Jones model is utilized to estimate binary diffusion coefficients. Wherever possible the input parameters are retained from the parent models. Otherwise collisional diameter and energy well depth parameters have been estimated largely based on those recommended in a review conducted by Mourits et al. [24], and correlated to molecular weight in a similar manner to Wang and Frenklach [25] by Dooley et al. [26]. The detailed model construction is composed of 2051 species and 8438 reactions.

Motivations and Objectives

The present technological paradigm to achieve a feasible quantitatively accurate capacity to numerically model the combustion behavior of real liquid transportation fuels on a flexible fuel basis in computational fluid dynamics simulations, involves a three-step strategy of 1) surrogate fuel definition, 2) kinetic model construction and 3) kinetic model reduction. The motivation of this study is to demonstrate the accuracy of the combined state of the art ability to realize this strategy.

The objectives of the present study are thus:

1) To demonstrate the performance of the detailed model in reproducing the available shock tube ignition delay and laminar burning velocity data available for each surrogate fuel component. In this manner, the model may then be tested against data from more complex mixtures with confidence.
2) To demonstrate the performance of the detailed model in reproducing the available shock tube ignition delay and laminar burning velocity data available for both the 1st and 2nd generation POSF 4648 surrogate fuels.
3) To ascertain the effectiveness of kinetic model reduction techniques in minimizing the model size that will allow for reasonable reproduction of the shock tube ignition delay and laminar burning velocity data available for both the 1st and 2nd generation POSF 4648 surrogate fuels.

Kinetic Model Reduction

Even for the idealized one dimensional flame geometries considered for kinetic model testing, as here, a certain level of model reduction from the highly detailed parent model is a prerequisite. Model reduction techniques are essential, not just to reduce computational costs but also to reduce the numerical stiffness associated with such a large number of conservation equations for broad classes of independent fuel chemistries and reaction pathways. When performing model reduction to ascertain detailed model performance, great care has been taken to ensure that the reduced model computations retain fidelity to those of the detailed parent model.

The Path Flux Analysis (PFA) kinetic model reduction scheme [27] has been utilized in this study. The procedure to produce reduced models first involves obtaining a numerical database of time dependent detailed chemical species profiles computed by the detailed model under homogenous constant volume

ignition delay conditions (as described below). Subsequently, a second speciation database is constructed under steady-state perfectly stirred reactor conditions.

For the objective of ascertaining the performance of the detailed model under flame conditions for each surrogate fuel component, after inspection of the target datasets, both databases are populated by considering conditions of: fuel/air mixtures of equivalence ratio of 0.6, 1.0 and 1.5, at 1atm and temperatures of 1000 K, 1200 K, 1500 K, and 1800 K. It is important to note that the choice of target conditions that define the reduction process, is a decision (or an assumption) made by the user. Thus it should be regarded as a source of uncertainty in the reduced model. Although the PFA method and other reduction schemes **[**e.g. 28, 29] can produce reduced models of sizes that are applicable to the geometry calculation of a flame (<500 species), the limitations of these approaches in terms of how smaller reduced models can be produced without losing the "true" fidelity of the parent model has not been fully addressed. In order to discuss this issue, a range of reduced models for each fuel component have been generated by exercising the PFA "fidelity threshold" value incrementally from 0.05 to 0.35.

This procedure is followed specifying each surrogate component individually (n-decane, iso-octane, toluene, n-dodecane, iso-octane, 1,3,5-trimethyl benzene and n-propyl benzene) as the fuel to produce the range of reduced models presented in Table 1, models #1-23. By testing the entire range of reduced models for each individual surrogate fuel component, the minimum model size to deviate in performance is identified, thus indicating an invalid reduction.

In the case of reduced models for the 1st and 2nd generation surrogate fuels, the goal is to provide working reduced models valid across both broad and narrower ranges of conditions. Thus, for these purposes, the entire database from low to high temperatures (700 K, 800 K, 900 K, 1000 K, 1200 K, 1500 K and 1800 K) and pressures (1 atm and 20 atm) is utilized, separately specifying each surrogate composition as the fuel. The reduced model size is then modulated only by varying the fidelity threshold value incrementally from 0.05 to 0.4.

These procedures produce the list of reduced models presented in Table 1.

Model #	Fuel	Species #	Short Name
1	iso-octane	127	ic8_127
2	iso-octane	157	ic8_157
3	iso-octane	352	ic8_352
4	iso-octane	494	ic8_494
5	iso-octane	509	ic8_509
6	n-decane	79	nc10_79
7	n-decane	118	nc10_118
8	n-decane	141	nc10_141
9	n-decane	441	nc10_441
10	n-dodecane	88	nc12_88
11	n-dodecane	118	nc12_118
12	n-dodecane	152	nc12_152
13	n-dodecane	215	nc12_215
14	n-dodecane	542	nc12_542
15	n-propyl benzene	171	npb_171
16	n-propyl benzene	351	npb_351
17	Toluene	138	Tol_138
18	Toluene	175	Tol_175
19	Toluene	351	Tol_351
20	1,3,5-trimethyl benzene	135	tmb_135
21	1,3,5-trimethyl benzene	156	tmb_156
22	1,3,5-trimethyl benzene	212	tmb_212

23	1,3,5-trimethyl benzene	352	tmb_352
24	1st generation Jet-A POSF 4658 Surrogate	144	1gen_144
25	1st generation Jet-A POSF 4658 Surrogate	167	1gen_167
26	1st generation Jet-A POSF 4658 Surrogate	211	1gen_211
27	1st generation Jet-A POSF 4658 Surrogate	233	1gen_233
28	1st generation Jet-A POSF 4658 Surrogate	348	1gen_348
29	1st generation Jet-A POSF 4658 Surrogate	461	1gen_461
30	1st generation Jet-A POSF 4658 Surrogate	651	1gen_651
31	1st generation Jet-A POSF 4658 Surrogate	1154	1gen_1154
32	2nd generation Jet-A POSF 4658 Surrogate	219	2gen_219
33	2nd generation Jet-A POSF 4658 Surrogate	231	2gen_231
34	2nd generation Jet-A POSF 4658 Surrogate	315	2gen_315
35	2nd generation Jet-A POSF 4658 Surrogate	384	2gen_384
36	2nd generation Jet-A POSF 4658 Surrogate	402	2gen_402
37	2nd generation Jet-A POSF 4658 Surrogate	425	2gen_425
38	2nd generation Jet-A POSF 4658 Surrogate	558	2gen_558
39	2nd generation Jet-A POSF 4658 Surrogate	695	2gen_695
40	2nd generation Jet-A POSF 4658 Surrogate	810	2gen_810
41	2nd generation Jet-A POSF 4658 Surrogate	965	2gen_965
42	2nd generation Jet-A POSF 4658 Surrogate	1291	2gen_1291

Table 1. List of reduced kinetic models, number of species and model short names, where the 1st generation Jet-A POSF 4658 Surrogate is a 42.7/33.0/24.3 mole % mixture of n-decane/iso-octane/toluene and the 2nd generation Jet-A POSF 4658 Surrogate is a 40.41/29.48/7.28/22.83 mole % mixture of n-dodecane/iso-octane/1,3,5-trimethyl benzene/n-propyl benzene.

Kinetic Model Simulations

All modelling simulations are conducted with a modified CHEMKIN II solver. Shock tube simulations are zero-dimensional and begin at the onset of the reflected shock period. Constant volume and homogeneous adiabatic conditions are assumed behind the reflected shock wave, consistent with the experimentally observed pressure profiles in [12-13 35, 39]. The reflected shock pressure and temperature are input as the initial pressure and temperature respectively. The simulated ignition delay time is defined consistent with the diagnostic utilised in each particular set of experiments.

Laminar burning velocities are calculated by simulating freely propagating flames using the PREMIX module with the mixture averaged transport model. Simulations were performed over a constant domain size. The use of at least 900-1300 grid points for each computation of each model assured that increments of at least 0.04 for both CURV and GRAD are met and that the reported solutions are sufficiently resolved to be practically independent of grid size. In addition, the computation of a valid solution is verified by confirming that the computed peak flame temperature is equivalent to the adiabatic flame temperature of each respective flame. For the pure component reduced models presented below, peak flame temperatures are always within at most +/- 10 K of the adiabatic flame temperature at constant pressure. The laminar burning velocity computations reported are estimated to be within +/- 0.5 cm/s of the true (grid independent) solution.

At the outset of this study it is recognized that numerical calculations of the combustion process in practical combustor geometries under flowing conditions requires significant large memory allocations due to the complexity associated with mass transport and heat transfer amongst large thermal gradients, much more so when the chemical model size is large. Considering this intended application, a mixture averaged transport model is more desirable than the alternative multicomponent description as it is

computationally much less expensive. Thus we have chosen to evaluate model performance against experiment with this transport description even though it is less fundamentally accurate than alternatives, recognising that calculations with a multicomponent transport approach and treatment of thermal diffusive effects will result in burning velocities generally 1-2 cm/s lower than those reported here.

III. Results and Discussions

At the outset, it is emphasized that the calculations presented below are the results of the hierarchical model strategy exactly as described above, which we consider to fairly approximate the state of the art (see [14, 15, 16]). At this time, absolutely no adjustments have been made to any parameters of the adopted submodels in order to produce improved performance. As such, the comparisons presented below may be viewed as genuine tests of predictability.

Detailed Model Performance in a Homogeneous System: Ignition Delay Time

Firstly, the performance of the fully detailed model (2051 species and 8438 reactions) against shock tube ignition delay measurements available for each surrogate fuel component is ascertained. In order to identify any delinquencies in performance due to the adoption of fuel subcomponent models into the specific hierarchical scheme described above, where possible and relevant, the calculations of the adopted (parent) model are also presented. As established below, no important deviations are noted.

A. **iso-octane Shock Tube Ignition Delay**

Figure 1 presents comparison of the iso-octane reflected shock ignition delay data available in the Stanford Database **[30-33]** to the computations of the detailed model. This collection of experimental data spans the high temperature regime (1177-2009 K), low to moderate pressures (1.1-8.7 atm) for fuel dilute test mixtures (0.01-1.0% iso-octane), oxygen concentrations spanning 0.125-12.5 %, corresponding to equivalence rations of 0.25-2.0. As the data set is large (95 individual experiments), for convenience it is presented below as a function of case number. Also presented are computations of the model of Mehl et al. [23], from which the iso-alkane chemistry of the detailed model presented here is derived. Statistical analysis of the data comprising Figure 1 reveals that the ignition delays computed by the detailed model presented in this work are on average 57.7 % longer than experiment, whereas the parent model of Mehl et al. is similarly an average of 54.9 % longer than experiment. This comparison demonstrates the accuracy in computation of the iso-octane high temperature ignition delay. It is also apparent that any differences in small species chemistry and any higher hydrocarbon coupling in the kinetic model of this study compared to the parent model of Mehl et al., results in no significant differences in the ignition delay computations of these iso-octane/oxidizer mixtures.

B. **n-decane Shock Tube Ignition Delay**

Figure 2 compares the performance of the detailed model of this study, to that of the "parent" higher n-alkane model of Westbrook et al. and also to the available shock tube experimental measurements of n-decane ignition delay. There are three independent studies in the literature which present stoichiometric fuel-in-air measurements of n-decane ignition at elevated pressures of 11-80 atm. From Figure 2, it can be observed that there are no significant differences in the calculations of the respective models, more particularly both models capture the quality phenomenological dependence of the ignition delay on temperature and pressure. However is it apparent that both models deviate from experiment quantitatively. More careful study shows that the disparity is as much as a-factor-of-three at lower temperatures, the magnitude of the deviation generally peaking at the end of negative temperature coefficient behavior. Performance is generally improved at higher temperature conditions, approaching 1300 K. It is notable that significant scatter appears amongst the individual data sets for comparable conditions. For example, for the 11 atm data of Pfhal et al. [36] and the 13 atm data of Zhukov et al. [34]

and Shen et al. [35] at ~1225 K, there appears to be differences larger than a factor of two in the reported ignition delay for these energy-dense, stoichiometric fuel-in-air mixtures.

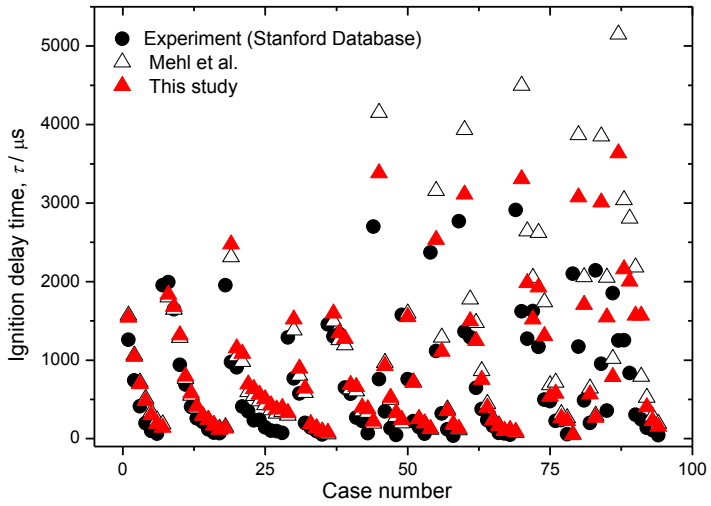

Figure 1. Shock tube ignition delay times for iso-octane/oxidizer mixtures from the Stanford Database [30-33], calculations with the detailed model of this study (red triangles) and calculations with the iso-octane model of Mehl et al. [23] (hollow triangles).

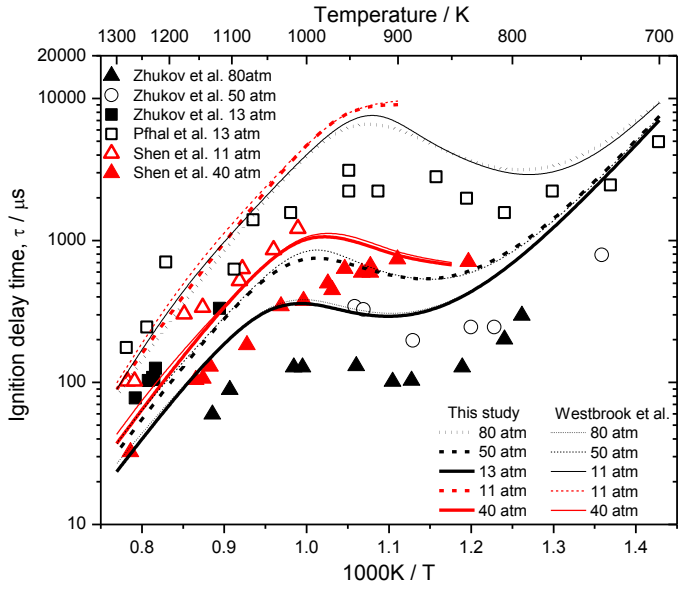

Figure 2. Shock tube ignition delay times for stoichiometric fuel in air mixtures of n-decane 80 atm [34], 50 atm [34] , 40 atm [35] 13 atm [36], and 11 atm [35]. Calculations with the detailed model of this study ("This study") and calculations with the model of Westbrook et al. [22] are shown as lines.

C. n-dodecane Shock Tube Ignition Delay

Vasu et al. [37] and Shen et al. [35] have reported measurements of the n-dodecane ignition delay time at equivalence ratios of 0.5 and 1.0 for fuel in air mixtures of n dodecane. The performance of both the detailed model of this study and that of the Westbrook et al. n-alkane model is evaluated against the measurements of Vasu et al. in Figure 3. Firstly, it is noted that some modest disparity is evident between the two models in the 700-950 K temperature range at these conditions. Moreover, a similar character in the comparison of model(s) to experiment as is evident in the n-decane comparison, is apparent in these n-dodecane tests. At almost all conditions, the models compute ignition delays that are approximately a factor of two longer than measured, even at high temperatures, where it is noted that the performance against n-decane ignition delay is somewhat improved relative to that at lower temperatures. Though not show here, the equivalent comparisons against the n-dodecane data of Shen et al. [35] have also been performed, and display similar behavior in terms of model performance. The parent n-alkane model (Westbrook et al.) is among the most detailed n-alkane kinetic models available. It is noted that this model was evaluated as being the best performing model, and amongst a group of three well performing kinetic models, when tested against detailed temporal speciation profiles from the Princeton variable pressure flow reactor [38]. Indeed, these were major reasons for the adoption of this model in the present study.

We return to the potential importance of these disparities when discussing the detailed model performance in simulation of 1st and 2nd generation POSF 4658 surrogate ignition delay.

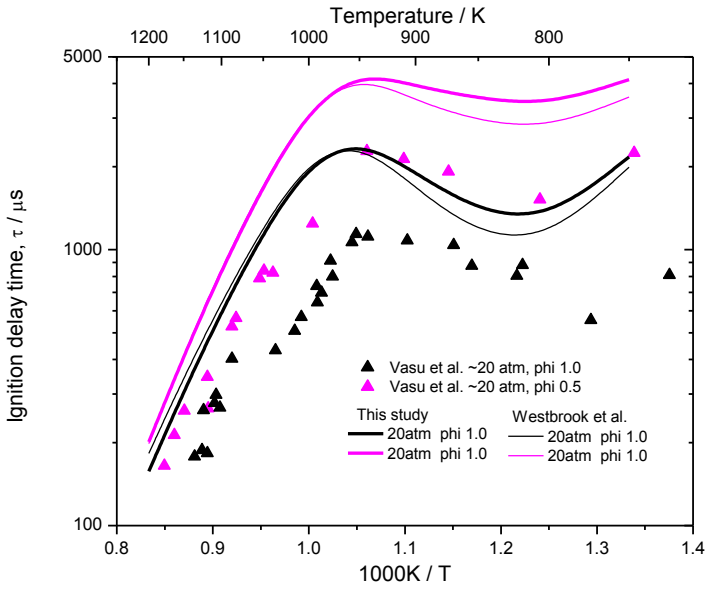

Figure 3. Shock tube ignition delay times for fuel in air mixtures of n-dodecane ~20 atm for equivalence ratios of 1.0 and 0.5 ~. Calculations with the detailed model of this study ("This study") and calculations with the model of Westbrook et al. [22] are shown as lines.

D. n-propyl benzene Shock Tube Ignition Delay

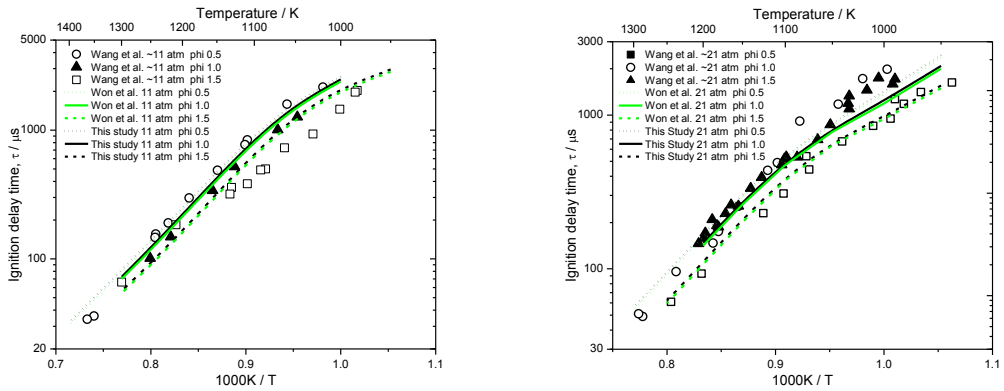

Figure 4. Shock tube ignition delay times for fuel in air mixtures of n-propyl benzene at ~11 atm and ~20 atm for equivalence ratios of 0.5, 1.0 and 1.5 from Wang et al. [39]. Calculations with the detailed model of this study ("This study") and calculations with the model of Won et al. [16] are shown as lines.

The parent model for the n-propyl benzene chemistry incorporated into the fully detailed surrogate fuel model is that of Won et al. **[**16]. It has been tested against diffusion flame extinction limits and separately against reflected shock ignition delay data from Wang et al. **[**39]. The performance of the detailed model of this study and that of the parent Won et al. **[**16] model is shown in Figure 4 against the data of Wang et al.. It is apparent that the respective dependencies of ignition delay on equivalence ratio, pressure and temperature are captured by the model to near quantitative accuracy. Note that any differences in the computations of each mode are barely discernible. This is unsurprising as the detailed model presented here has at as its core the entirely self-consistent aromatic submodels of n-propyl benzene, 1,3,5- trimethyl benzene and toluene. These models are implicitly compatible with the small species chemistry submodels used in this work, as the supporting works of Won et al., **[**16] Diévart et al., **[**17] and Metcalfe et al. **[**15], use the very same submodel. Thus the only potential for adulteration from the performance from that which has already been demonstrated in those studies, is the occurrence of any complicating effects due to the additional presence of n-alkane and iso-alkane chemistry.

Similar tests have been performed against the shock tube ignition delay presented in Metcalfe et al. [15] for the case of toluene and very recently by Diévart et al. [16] for the case of 1,3,5-trimethyl benzene. Those comparisons of the ignition delay calculated by the respective parent model to those calculated by the detailed model of this study bare very similar resemblance to those for the case of n-propyl benzene above. As the data sets are rather vast for the case of toluene, they have not been included here.

E. **Jet-A POSF 4658 Shock Tube Ignition Delay**

Having established the performance of the detailed model against surrogate component ignition delay data. Figure 5 presents the ignition delays computed by the detailed model for both the "1st generation" Jet-A POSF surrogate fuel, (n-decane/iso-octane/toluene, 42.7/33.0/24.3 mole %) and the more complex "2nd generation" Jet-A POSF 4658 surrogate fuel (n-dodecane/iso-octane/1,3,5 trimethyl benzene/n-propyl benzene 40.41/29.48/7.28/22.83 mole %). We have previously demonstrated that both of these mixtures closely share the premixed combustion phenomena of the target real Jet-A fuel, POSF 4658, such shock tube ignition delay data is also included in Figure 5 for reference. It is observed that the calculated ignition delays for both mixtures are always within approximately a factor-of-two of experiment in all cases, and often agree more closely with the measurement. Moreover the calculated

ignition delays for both fuels are extremely similar, only showing significant difference of approximately 20% at the temperatures corresponding to the end of the NTC region.

This level of performance is apparently in contrast to the performance of the same detailed model against the n-alkane ignition delay times, where discrepancies of factors-of-two to factors-of-three are apparent even in the high temperature regime. In simulation of the multi component surrogate fuels, above 1000 K, the detailed model shows ignition delays that are just ~70% longer than experiment for the 1st generation surrogate composition, and only ~50% longer for the 2nd generation surrogate composition.

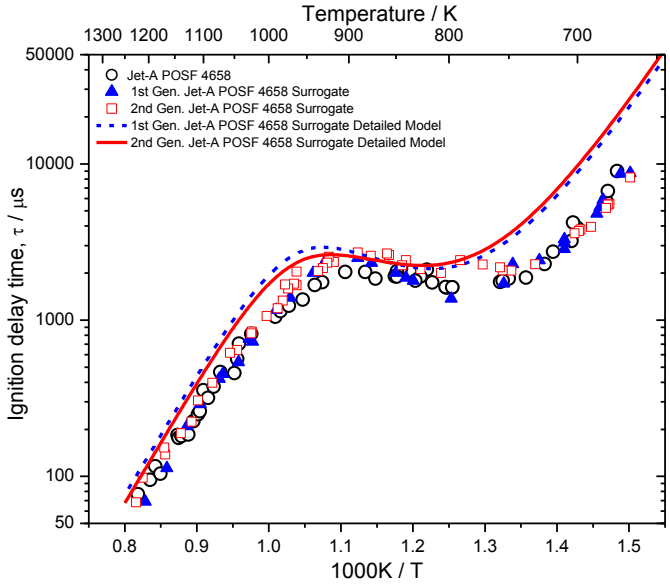

Figure 5. Ignition delay times for stoichiometric fuel-in-air mixtures of Jet-A POSF 4658 [12] (circles) at 16-25 atm, 1st generation [12] (n-decane/iso-octane/toluene 42.7/33.0/24.3 mole %, triangles, dashed line) and 2nd generation [13] (n-dodecane/iso-octane/1,3,5 trimethyl benzene/n-propyl benzene 40.41/29.48/7.28/22.83 mole %, squares, solid line) POSF 4658 surrogate fuels. Symbols are experiment [12-13], lines are computations of the detailed model of this study.

Reduced Model Performance in a Flame Geometry: Laminar Burning Velocity

Several reduced models are produced to test flame performance as described by Table 1. The motivation to produce several models for the same purpose but of varying dimension is to provide some confidence that the model computations are fundamental in nature, predictive and not adversely effected by over reduction.

A. **iso-octane Laminar Burning Velocity**

The laminar burning velocities of iso-octane/air mixtures of equivalence ratios of 0.7-1.5 at 1 atm and an unburned gas temperature of 298 K are computed at various levels of detail and shown in Figure 6. An important body of experimental measurements of the iso-octane laminar burning velocity using different measurement techniques has accumulated for this condition in the literature. The data are also shown in Figure 6. It can be seen that each of the reduced models reproduce the main body of experimental data reasonably well, deviating from each other only at species numbers less than 150, indicative that the

performance of models of species number 352, 494 and 509 is likely to closely approximate the true performance. It is noted that while the reduced models accurately track experiment at both fuel-lean and fuel-rich equivalence ratios, where the burning velocities are lower, the consensus peak burning velocity at this condition, 35.8 cm/s, is ~2.5 cm/s higher than estimated by the models.

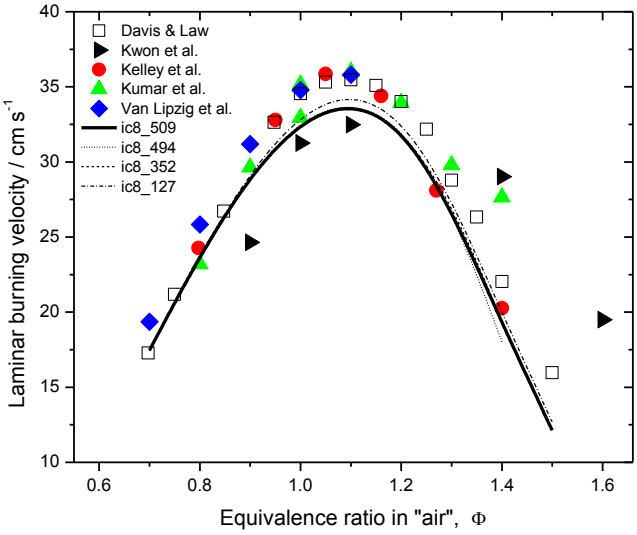

Figure 6. Laminar burning velocities for mixtures of iso-octane/air at 1 atm and 298 K [40-44] (symbols) and computations with reduced models of this study (lines).

B. n-decane Laminar Burning Velocity

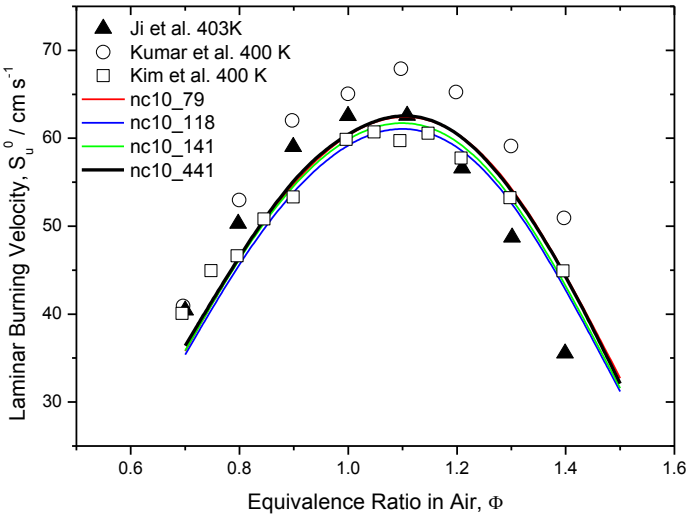

Figure 7. Laminar burning velocities for mixtures of n-decane/air at 1 atm and ~400 K [45-47] (symbols) and computations with reduced models of this study (lines).

Figure 7 compares the calculations of four of the n-decane reduced models of Table 1 to laminar burning velocity measurements available for 1 atm and ~400 K. First, it is important to note that in contrast to the iso-octane scenario, the consensus on the exact laminar burning velocity of n-decane across these equivalence ratios is less precise. Here it can be seen that the largest reduced model of 441 species captures the peak burning velocity data of Ji et al. **[**46] and Kim et al. **[**47] very closely, the data of Kumar et al. **[**45] being disparate at some ~7 cm/s higher. Furthermore, for the burning velocities of this surrogate fuel component, there is close consensus between each reduced model, where the maximum total deviation is ~1 cm/s. At high equivalence ratios, the model computations lie between the bounds of the experimental data, and agree quite closely with the recent data of Kim et al. **[**47]. At lean equivalence ratios, the model again most closely follows the data of Kim et al., however it is noted that this data set lies four to five cm/s lower than that of Ji et al. and approximately a further 1 cm/s lower than the data of Kumar et al. At the lowest equivalence ratio reported, there is general consensus amongst each set of experiments, where the models compute a burning velocity of ~36.5cm/s, experiment presents a consensus of ~40 cm/s.

C. **n-dodecane Laminar Burning Velocity**

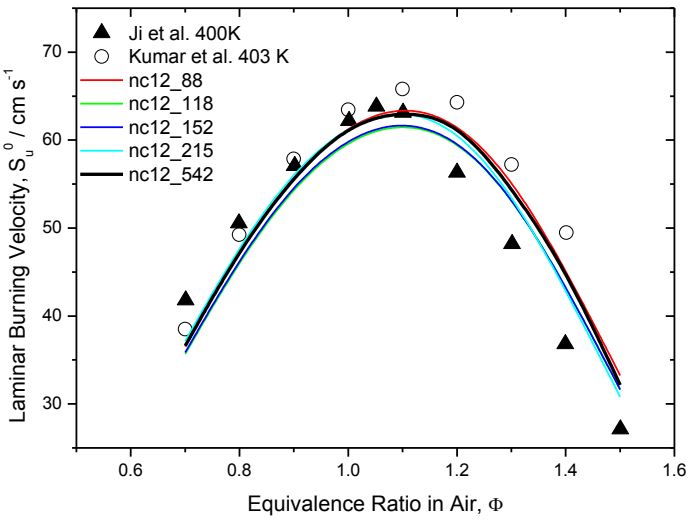

Figure 8. Laminar burning velocities for mixtures of n-dodecane/air at 1 atm and ~400 K [45, 46] (symbols) and computations with reduced models of this study (lines).

Kumar et al. [45] and Ji et al. [46] also present measurements of n-dodecane laminar burning velocity. Their data is shown in Figure 8, with the computations the five reduced models from Table 1 pertinent to n-dodecane. Evaluation of the model performance presents a similar scenario to that discussed above for the case of n-decane. The calculations of all models are consistent to within ~1 cm/s. This step wise decrease in fidelity occurs for reductions below 215 species. The largest reduced model contains 542 species and its computations locate, either within the spread of experimental data, or at lean conditions, approximately 2 cm/s lower that experiment.

D. **n-propyl benzene Laminar Burning Velocity**

The calculations of the reduced models produced for n-propyl benzene of 171 and 351 species are presented in Figure 9 against the burning velocity data determined experimentally by Ji et al. [48] at 353 K and 1 atm. Figure 9 shows both models to be consistent to within less than 1 cm/s at all conditions.

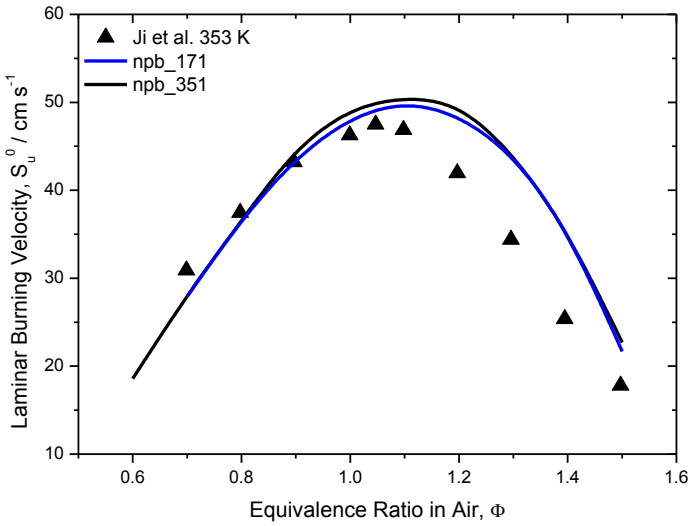

Figure 9. Laminar burning velocities for mixtures of n-propyl benzene/air at 1 atm and ~353 K [48] (symbols) and computations with reduced models of this study (lines).

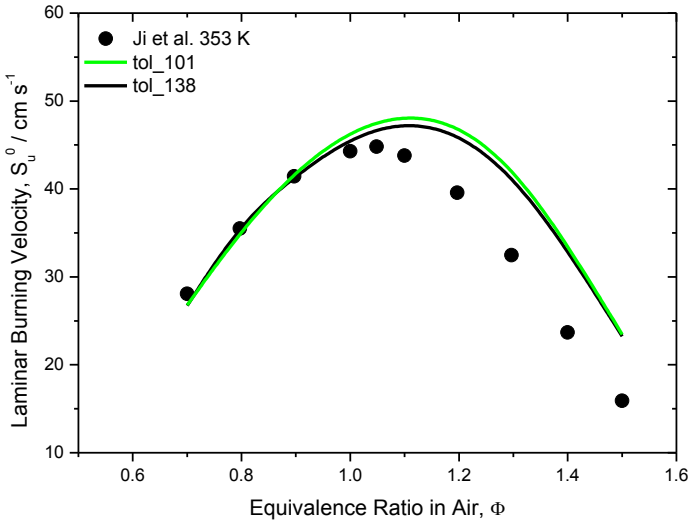

Figure 10. Laminar burning velocities for mixtures of toluene/air at 1 atm and ~353 K [48] (symbols) and computations with reduced models of this study (lines).

The entire aromatic submodel is much smaller than that of the alkane components, the toluene, n-propyl benzene and 1,3,5-trimethyl benzene submodels contain 329, 353 and 454 species respectively, compared to a total of 2051species for the detailed model. This allows for much smaller reduced models

of high fidelity to be produced for the aromatic fuel components than for those large alkane fuel components. From Figure 9, it is apparent that while the peak burning velocities and the values at lean conditions are adequately computed by the reduced models, the experimental values at rich equivalence ratios is somewhat over estimated. Similar was noted in the independent analysis of the parent n-propyl benzene model [16] presented by Ji et al. [48].

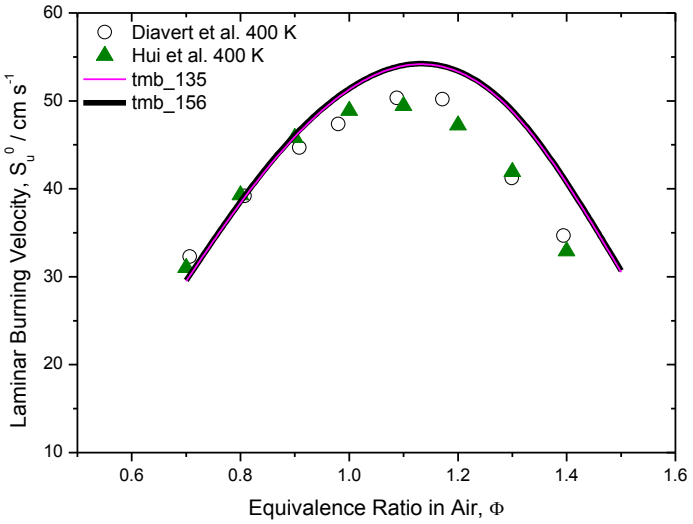

Figure 11. Laminar burning velocities for mixtures of 1,3,5-trimethyl benzene/air at 1 atm and 400 K [17, 49] (symbols) and computations with reduced models of this study (lines).

E. Toluene Laminar Burning Velocity

A very similar scenario to that presented for n-propyl benzene is apparent from Figure 10 for the case of toluene. Both detailed models agree very closely and with the experimentally determined burning velocities at fuel lean and stoichiometric conditions. However a similar over estimation is apparent under fuel rich conditions.

F. 1,3,5-trimethyl benzene Laminar Burning Velocity

The results and discussions for 1,3,5-trimethyl benzene burning velocities parallel those for toluene and n-propyl benzene, with the notable difference that the peak burning velocity is over estimated by ~ 4 cm/s.

Here follows a summary of the performance tests of the kinetic model described in this study to reproduce the pure component laminar burning velocity data for the components of the surrogate fuel formulation palette: iso-octane burning velocities are shown to be reproducible to a maximum deviation of negative 2.5 cm/s (7 %); n-decane, and n-dodecane burning velocities are reproducible to a maximum deviation of negative 4 cm/s (~ 10%) which in both cases, occurs at the leanest equivalence ratio; the burning velocities of the aromatic functionalities is quantitatively reproduced at fuel lean and stoichiometric equivalence ratios, but is consistently over estimated for each aromatic component at fuel rich conditions, in some cases by up to positive 20%.

Reduced Model Performance Against Jet-A POSF 4658 Combustion Properties via Surrogate Fuels

Having established the performance of the kinetic model construction at the pure component level for the test combustion properties of ignition delay, and laminar burning velocity, the following section describes the production of reduced models for the 1st and 2nd generation POSF 4658 Jet-A surrogate fuel compositions. The performance of these reduced models against both the detailed model from which they are derived and to the experimental data reported for each surrogate fuel in [12] and [13] is described.

For the 1st generation n-decane/iso-octane/toluene 42.7/33.0/24.3 mole % composition a total of nine reduced models ranging from 144-1154 species are produced. Their performance is compared to that of the detailed model and to experimentally measured shock tube ignition delay data for this composition and that of Jet-A POSF 4658 in Figure 12 . For reference, factor of two positive and negative thresholds of the ignition delay calculated by the detailed model are provided by uncertainty bars. From Figure 12, a minimum model size of 233 species is required to even qualitatively reproduce the entire temperature dependence of the ignition delay curve. The reduced models of less than 233 species, fail to capture the low temperature reactivity and begin to deviate noticeably from the detailed model performance at temperatures as high as 1100 K. However, the calculations of these smaller models do closely track the detailed model performance at the highest temperatures. At temperatures of ~ 1000 K, at these 20 atm conditions, the reduced models of less than 233 species compute ignition delays that are more than a factor of two disparate (longer) than those of the detailed model.

In contrast, at all conditions analysed, all reduced models of greater than 233 species consistently compute ignition delays that are well within the arbitrarily assigned factor of two precision threshold. In the acute numerical sense, the smallest valid reduction is that of 651 species. This model closely tracks the computations of its parent detailed model. Subsequent reductions, deviate in performance noticeably from the detailed model in the low temperature regime between 800-900 K. In this region it is noted that model performance behaves in a non-linear manner according to the level of reduction. For example, the 233 species reduction, computes ignition delays which are of intermediate values to those computed by the 651 species reduced model and the 348 species reduced model. Thus, for example, while the performance of 1Gen_233 may be judged by the user to be adequate against this particular set of conditions, from a numerical perspective the model is less valid the larger 2Gen_348.

A. **Jet-A POSF 4658 Ignition Delay Time**

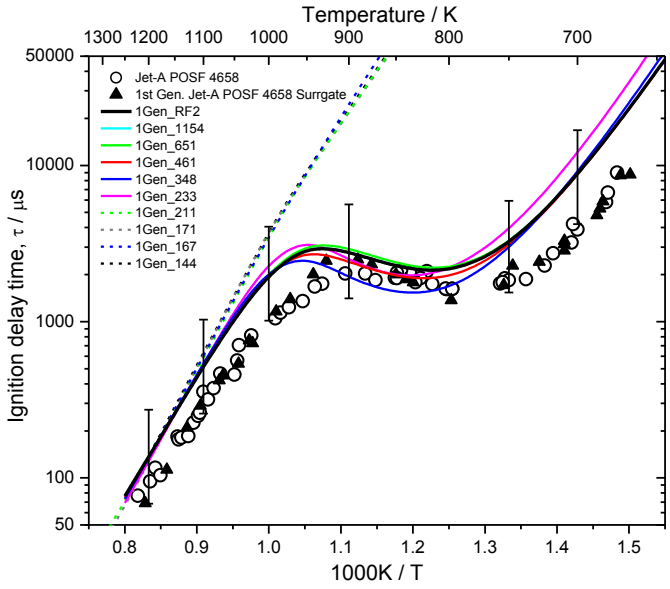

Figure 12. Shock tube ignition delay times for stoichiometric fuel in air mixtures of Jet-A POSF 4658 (hollow circles, 16-25 atm [12]) and the 1st generation (n-decane/iso-octane/toluene 42.7/33.0/24.3 mole %) Jet-A POSF 4658 surrogate fuel (solid triangles, 17-23 atm [12]). Lines are simulations with the kinetic models of this study. Error bars show a factor-of-two threshold to the computations of the detailed model.

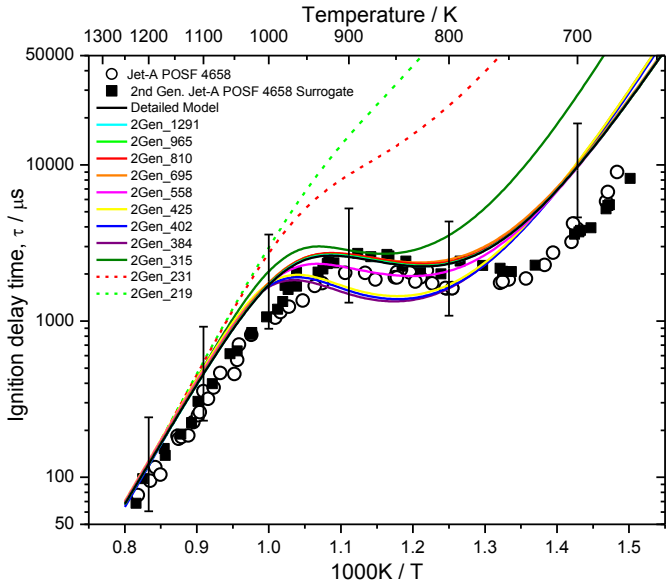

Figure 13. Shock tube ignition delay times for stoichiometric fuel in air mixtures of Jet-A POSF 4658 (hollow circles, 16-25 atm [12]) and the 2nd generation (n-dodecane/iso-octane/1,3,5-trimethyl benzene/n-propyl benzene 40.41/29.48/7.28/22.83 mole %) Jet-A POSF 4658 surrogate fuel (solid squares, 17-22 atm [13]). Lines are simulations with the kinetic models of this study. Error bars show a factor-of-two threshold to the computations of the detailed model.

For the case of the 2nd generation n-dodecane/iso-octane/1,3,5-trimethyl benzene/n-propyl benzene 40.41/29.48/7.28/22.83 mole % composition, the larger dimensional size of this model (larger molecular weight components, more species, more reactions etc.) leads to a number of potentially important differences from the scenario of the smaller 1st generation composition discussed above. Firstly, a larger number of reduced models is produced by exercising the same reduction procedure. In all, a total of eleven reduced models are produced and their calculated ignition delay times are presented in Figure 13 in an identical scenario to that of Figure 12. Secondly, the smallest reduced model that quantitatively captures the entire temperature dependence of the ignition delay consists of 315 species, 82 species larger than the equivalent reduced model for the 1st generation composition. It is also noted, that the fidelity of the reduced models of similar size for the 1st generation composition is much higher than those for the 2nd generation composition. For example, compare the performance of 1Gen_348 with 2Gen_315. These penalties highlight the importance of choosing the smallest surrogate composition possible for the intended scenario, e.g. premixed versus non premixed combustion. Obviously, from the findings presented previously [13], it is expected that reduced models derived from the 2nd generation composition will perform better than those derived from the 1st generation composition under conditions dominated by mass diffusion.

B. Jet-A POSF 4658 Laminar Burning Velocity

Figures 12 and 13 demonstrate that the employed reduction procedure, and the fidelity of the detailed model presented here, are in combination capable of producing reduced order models of ~200-300 species that reproduce the experimentally observed ignition behavior of jet aviation fuels to well within a factor-of-two at most conditions. Figures 14 and 15 present the equivalent comparisons for the case of the laminar burning velocities measured for Jet-A POSF 4658 and both the 1st and 2nd generation Jet-A POSF 4658 surrogate fuel compositions.

Figure 14, shows that the four tested reduced models for the 1st generation composition agree with one another to within ~1.5 cm/s, for models containing 133, 167, 211 and 461 species. Note that 1Gen_461 (Figure 12) retains close fidelity to the detailed parent model, and experiment, throughout the entire low and high temperature range (600-1300K). However, all tested models fail to reproduce the measured laminar burning velocity of the n-decane/iso-octane/toluene 42.7/33.0/24.3 mole % composition with quantitative accuracy. Model computations are lower than experiment by ~6-9.5 cm/s across the equivalence ratio range 1.1 ~ 0.7. From Figure 15, test calculations with a large reduction of the 2nd generation composition, 2Gen_425, which also satisfies the entire temperature range of ignition delay measurements, shares closely the computed laminar burning velocities of the reduced models for the 1st generation compositions. It is noted that the performance of these reduced models versus surrogate fuel laminar burning velocities is more disparate from experiment that what has been demonstrated for any of the constituent surrogate fuel components.

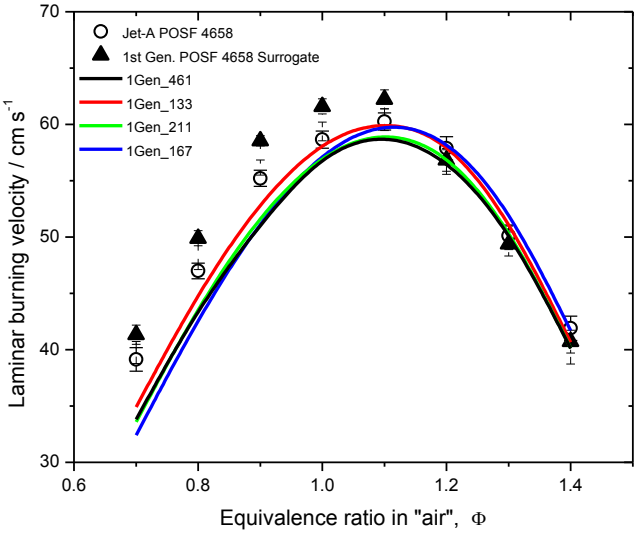

Figure 14. Jet-A POSF 4658 and 1st generation (n-decane/iso-octane/toluene 42.7/33.0/24.3 mole %) Jet-A POSF 4658 surrogate fuel laminar burning velocities at 1 atm and 400 K [13] (symbols) and computations with reduced models of this study (lines). Burning velocities are obtained by the non-linear extrapolation technique as to appear in Hui & Sung FUEL [personal communication C. J. Sung 2012 University of Connecticut].

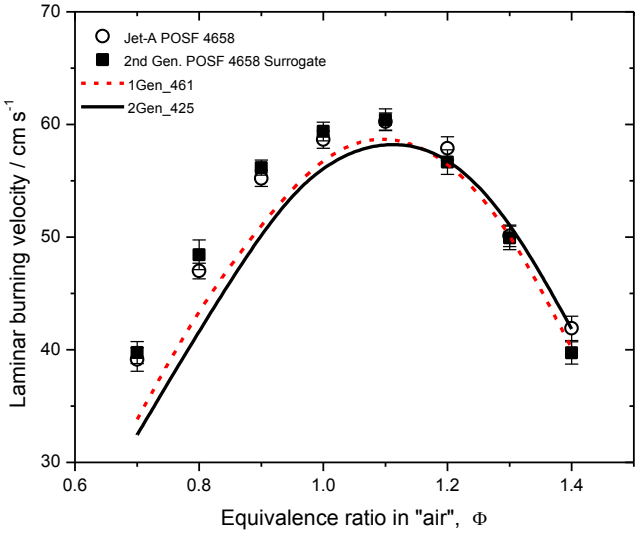

Figure 15. Jet-A POSF 4658 and 2nd generation [13] (n-dodecane/iso-octane/1,3,5 trimethyl benzene/n-propyl benzene 40.41/29.48/7.28/22.83 mole %) Jet-A POSF 4658 surrogate laminar burning velocities at 1 atm and 400 K [13] (symbols) and computations with reduced models of this study (lines). Burning velocities are obtained by the non-linear extrapolation technique as to appear in Hui & Sung FUEL 2013 [personal communication C. J. Sung 2012 University of Connecticut].

IV. Concluding Remarks

The construction and performance of a detailed chemical kinetic model to describe the combustion properties of mixtures of n-decane, n-dodecane, iso-octane, toluene, 1,3,5-trimethyl benzene and n-propyl benzene as surrogate fuels for jet aviation fuels is described. The detailed model is entirely hierarchal and its performance is demonstrated at each surrogate component level for shock tube ignition delay and laminar burning velocity as initial tests of fidelity. For all surrogate components tested, it is shown that ignition delays calculated by the detailed model, and the parent literature model, for the tested n-alkanes are the most disparate from available experiments, sometimes deviating by approximately a factor-of-three. Model performance against aromatic and iso-octane ignition delays is much more favourable.

In contrast, experimental determinations of the normal and isomerised alkane laminar burning velocities are reproduced to within a largest deviation of ~4cm/s, corresponding to ~10%. For the aromatic surrogate fuel components, laminar burning velocities are reproduced to within 1 cm/s at lean equivalence ratios, but notable deviations of up to 10 cm/s are observed at rich equivalence ratios.

The detailed model reproduces shock tube ignition delay measurements of both surrogate fuels, and by extension jet-A POSF 4658, to within 70% and 40% of the ignition delay measured for the respective n-decane/iso-octane/toluene and n-dodecane/iso-octane/1,3,5 trimethyl benzene/n-propyl benzene surrogate fuels, at temperatures greater than ~800 K. A series of reduced models are produced for each surrogate compositions. Within the procedures exercised here, it is shown that reduced models must be composed of between ~200-350 species to reproduce the detailed model ignition delay across the entire 600-1300 K temperature range, depending on the surrogate fuel composition specified. Reduced models smaller than this, are shown to be applicable only to temperatures above 1100 K for the 20 atm conditions tested in this study. A selection of these reduced models is used to evaluate model performance against the burning velocity data measured for each surrogate fuel. It is found that the burning velocities at equivalence ratios higher than stoichiometric can be accurately reproduced. However in apparent contradiction of the burning velocity performance against individual surrogate components, for fuel lean conditions, the

models compute burning velocities that are approximately 25% lower than those measured. An explanation for this discrepancy is the subject of ongoing work. The detailed and reduced kinetic models presented in this work are available from the authors.

Acknowledgments

Work at University of Limerick is supported by Science Foundation Ireland under the Charles Parsons Energy initiative. Research performed at Princeton University was supported by an AFOSR MURI under grant number FA9550-07-1-0515. Work at University of South Carolina was supported by the College of Engineering and Computing.

References

1. Edwards T., Maurice L. Q., J. Prop. Power. 17 (2001) 461–466.
2. Wood C. P., McDonell V. G., Smith R. A., Samuelsen G. S., J. Prop. Power 5 (1989) 399–405.
3. Schulz W. D., American Chemical Society 37 (1992) 383–392.
4. Violi A., Yan S., Eddings E. G., Sarofim A. F., Granata S., Faravelli T., Ranzi E., Combust. Sci. Technol. 174 (2002) 399–417.
5. Ranzi E., Dente M., Bozzano G., Goldaniga A., Faravelli T., Prog. Energy Combust. Sci. 27 (2001) 99–139.
6. Guéret C., Cathonnet M., Boettner J.-C., Gaillard F., Proc. Combust. Inst. 23 (1990) 211–216.
7. Agosta A., Miller D. L., Cernansky N. P., Favarelli T., Ranzi E., Exp. Therm. Fluid Sci. 28 (2004) 701–708.
8. Cooke J. A., Bellucci M., Smooke M. D., Gomez A., Violi A., Faravelli T., Ranzi E., Proc. Combust. Inst. 30 (2005) 439–446.
9. Eddings E. G., Yan S., Ciro W., Sarofim A. F., Combust. Sci. Tech. 177 (2005) 715–739.
10. Dagaut P., El Bakali A., Fuel 85 (2006) 944–956.
11. Gokulakrishnan P., Gaines G., Klassen M. S., Roby R. J., Currano J., J. Eng. Gas Turb. Power 129 (2007) 655–664.
12. Dooley S., Won S. H., Chaos M., Heyne J., Ju Y., Dryer F. L., Kumar K., Sung C.-J., Wang H., Oehlschlaeger M. A., Santoro R. J., Litzinger T. A., Combust. Flame 157 (2010) 2333–2339.
13. Dooley S., Won S. H., Heyne J., Farouk T. I., Ju Y., Dryer F. L., Kumar K., Hui X., Sung C. –J., Wang H., Oehlschlaeger M. A., Iyer V., Iyer S., Litzinger T. A., Santoro R. J., Malewicki T., Brezinsky K., Combust. Flame 159 (2012) 1444–1466.
14. Dooley S., Won S. H., Jahangirian S., Ju Y., Dryer F. L., Wang H., Oehlschlaeger M. A., Combust. Flame, 159 (2012) 3014-3020.
15. Metcalfe W. K., Dooley S., Dryer F. L., Energy & Fuels 25 (2011) 4915–4936.
16. Won S. H., Dooley S., Dryer F. L., Ju Y., Proc. Combust. Inst. 33 (2011) 1163–1170.
17. Diévart P., Won S. H., Kim H. H., Ju Y., Dooley S., Dryer F. L., Wang W., Oehlschlaeger M. A., accepted to Fuel. (2012).
18. Li J., Zhao Z., Kazakov A., Chaos M., Dryer F. L., Scire Jr. J. J., Int. J. Chem. Kinet. 39 (2007) 109–136.
19. Zhao Z., Chaos M., Kazakov A., Dryer F. L., Int. J. Chem. Kinet. 10 (2008) 1–18.
20. Healy D., Curran H. J., Simmie J. M., Kalitan D. M., Zinner C. M., Barrett A. B., Petersen E. L., Bourque G., Combust. Flame 155 (2008) 441–448.
21. Laskin A., Wang H., Law C.K., Int. J. Chem. Kinet. 32 (2000) 589–614.
22. Westbrook C. K., Pitz W. J., Herbinet O., Curran H. J., Silke E. J., Combust. Flame, 156 (2009) 181–199.
23. Mehl M., Pitz W. J., Westbrook C. K., Curran H. J., Proc. Combust. Inst. 33 (2011) 193–200.
24. Mourits F. M., Rummens F. H. A., Can. J. Chem. 55 (1977) 3007–3020.
25. Wang H., Frenklach M., Combust. Flame 96 (1994) 163–170.
26. Dooley S., Uddi M., Won S. H., Dryer F. L., Ju Y., Combust. Flame 159 (2012) 1371–1384.

27. Sun W., Chen Z., Gou X., Ju Y., Combust. Flame 157 (2010) 1298–1307.
28. Lu T., Law C. K., Proc. Combust. Inst. 30 (2005) 1333–1341.
29. Niemeyer K. E., Sung C.-J., Raju M. P., Combust. Flame, Vol. 157 (2010) 1760–1770.
30. http://hanson.stanford.edu/researchReports/kinetics/Fundamental_Kinetics_Database_Volume_1.pdf
31. Oehlschlaeger M. A., Davidson D. F., Herbon J. T., Hanson R. K., Int. J. Chem. Kin. 36 (2004) 67–78.
32. Davidson D. F., Oehlschlaeger M. A., Herbon J. T., Hanson R. K., Proc. Combust. Inst. 29 (2002) 12995–1301.
33. Oehlschlaeger M. A., Davidson D. F., Herbon J. T., Hanson R. K., AIAA 2203–0830 (2003).
34. Zhukov V. P., Sechenov V. A., Starikovski A. Y., Combust. Flame 153 (2008) 130–136.
35. Shen H. P., Steinberg J., Vanderover J., Oehlschlaeger M. A., Energy & Fuels 23 (2009) 2482–2489.
36. Pfahl U., Fieweger K., Adomeit G., Proc. Combust. Inst. 26 (1996) 781–789.
37. Vasu S. S., Davidson D. F., Hong Z., Vasudevan V., Hanson R. K., *Proc. Combust. Inst.* 32 (2009) 173–180.
38. Jahangirian S., Dooley S., Dryer F. L., Combust. Flame 159 (2012) 30–43.
39. Wang H., Oehlschlaeger M. A., Dooley S., Dryer F. L., 7th U.S. National Technical Meeting of the Combustion Institute, Georgia Institute of Technology, Atlanta, GA March 20-23, 2011. `
40. Kwon O. C., Hassan M. I., Faeth G. M., J. Propul. Power 16 (2000) 513–522.
41. Kumar K., Freeh J. E., Sung C. -J., Huang Y., J. Propul. Power 23 (2007) 428–436.
42. Kelley A. P., Liu W., Xin Y. X., Smallbone A. J., Law C. K., Proc. Combust. Inst. 33 (2011) 501–508.
43. Davis S. G., Law C. K., Proc. Combust. Inst. 27 (1998) 521–527.
44. van Lipzig J. P. J., Nilsson E. J. K., de Goey L. P. H., Konnov A. A., Fuel 90 (2011) 2773–2781.
45. Kumar K., Sung C.-J., Combustion and Flame 151 (2007) 209–224.
46. Ji C., Egolfopoulos F. N., Proc. Combust. Inst. 33 (2011) 955–961.
47. Kim H. H., Won S. H., Santner J., Chen Z., Ju. Y., Proc. Combust. Inst. in press 2012.
48. Ji C., Dames E., Wang H., Egolfopoulos F. N., Combust. Flame 159 (2012) 1070–1081.
49. Hui X., Das A. K., Kumar K., Sung C.-J., Dooley S., Dryer F. L., Fuel 97 (2012) 695-702.